21st Australasian Fluid Mechanics Conference
Adelaide, Australia
10-13 December 2018

Dynamics of rotating horizontal convection with a moving heated surface

TzeKih Tsai[1], **Wisam K. Hussam**[2] **and Gregory J. Sheard**[1]

[1]The Sheard Lab, Department of Mechanical and Aerospace Engineering
Monash University, Melbourne, Victoria 3800, Australia
[2]School of Engineering, Australian College of Kuwait, Safat, Kuwait

Abstract

The dynamics of mechanically stressed rotating horizontal convection in a cylindrical enclosure is investigated numerically. The rotating cylindrical container has a differentially rotating base with a thermal forcing applied radially on the bottom boundary. The conditions on the other boundaries are thermally insulated. Axisymmetric numerical solutions showing a steady regime flanked by two unsteady regimes at both ends of the range of Rossby number investigated. The thermally direct mechanical forcing (positive Rossby number) enhances radially horizontal convection, whereas the thermally indirect (negative Rossby number) forcing reverses thermal gradient results in a heated region away from the edge of the container. A robust Nusselt number scaling of $\sim Q^{1/2}$ is observed at a high value of Rossby number for both thermally direct and indirect forcing.

Introduction

Rotating horizontal convection is a class of rotating flow where an uneven thermal forcing is imposed along a horizontal boundary. The combination of a horizontal convection and rotation has been studied in a rectangular enclosure [1, 11]. and a cylindrical enclosure [5, 8]. However, the effect of surface shear stresses on rotating horizontal convection has received less attention. Understanding the coupling of surface shear stresses and rotating horizontal convection flows is important in many industrial applications as well as in geophysical flows.

The effect of a surface stress on convection driven by non-uniform heating had been studied numerically [3, 10] as well as experimentally [12] in the context of ocean circulation. More recently, Hazewinkel *et al.* [4] concluded numerically that mechanical stirring enhanced horizontal convection which allowed surface heating to penetrate into greater depths. Ilicak *et al.* [6] and Stewart *et al.* [9] argued that mechanical forcing (i.e. winds and tides) were crucial to the maintenance of a deep stratification and to a mean flow beneath the oceans. These studies were confined to a non-rotating rectangular enclosure with non-uniform horizontal heating.

Barkan *et al.* [2] numerically investigated a rotating reentrant channel forced by horizontal buoyancy fluxes and wind stress. To date there has been no comprehensive study into the behaviours of rotating horizontal convection with systematic variation of an imposed surface shear stress in a cylindrical container. This motivates a detailed study into the dynamics of mechanically stressed rotating horizontal convection and forms the basis of the system considered in the present numerical study, a rotating cylindrical container, with a differentially rotating bottom boundary that has a radially increasing temperature profile. A key question in stressed rotating horizontal convection is the effect of surface shear stresses on the heat transfer characteristics of the flows.

In this study, a high-order spectral element solver is used to study horizontal convection within a cylindrical tank with a linear temperature profile imposed radially along the base which rotates at a differential rate to the tank rotation. Two control parameters are used in this investigation. The first of these is the rotation parameter (Q), which accounts for the importance of rotation in horizontal convection, it quantifies the square of the ratio between thermal boundary layer thickness and Ekman layer thickness. The other parameter is the Rossby number (Ro), which represents the differential rotation rate between the bottom base and the main rotating tank. A positive Rossby number indicates the base rotates faster than the tank and vice versa. Numerical solutions are obtained for rotation parameter of $1 < Q < 100$, Rossby number of $-1 < Ro < 1$ at a fixed Rayleigh number of 10^9 and a fixed Prandtl number of $Pr = 6.14$, representative of water. The flow dynamics and the effects of the Rossby number on the Nusselt number scaling will be investigated.

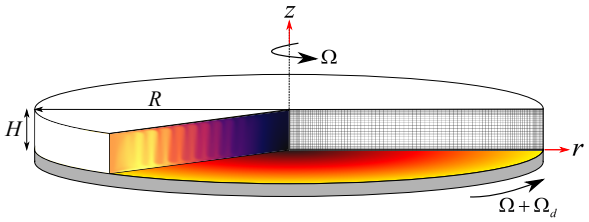

Figure 1. Schematic diagram shows a cross section of the computational domain of a cylindrical tank rotating at a rate Ω, with a linear temperature profile imposed radially along the base of the tank which rotates at a differential rate of $\Omega + \Omega_d$. The inset shows spatially discretised semi-meridional (z-r plane) mesh and temperature contours for $Q = 20$, $Ro = -0.5$ at a Rayleigh number of $Ra = 10^9$. The darker shade represents colder temperature and the lighter shade indicates hotter temperature.

Numerical Setup

A numerical setup consisting of a cylindrical tank filled with fluid having a Prandtl number of 6.14 is used to simulate the effect of a moving heated surface on rotating horizontal convection. The cylindrical tank has a radius R and a height H, as depicted in figure 1. The tank aspect ratio is $\Lambda = H/R = 0.16$.

The numerical simulations were conducted in cylindrical coordinates with a velocity field, $\boldsymbol{u}(z,r,\phi,t) = \langle u_z, u_r, u_\phi \rangle$. The tank rotation is described by imposing an azimuthal velocity on the top and side wall as $u_\phi = r\Omega$, where r is the radial coordinate. A differential rotation rate of $\Omega + \Omega_d$ is imposed on the heated base. No-slip boundary condition was enforced by imposing a zero normal ($u_z = 0$) and radial ($u_r = 0$) velocity on all solid boundaries. A linear temperature profile with an increase of $\delta\theta$ from $r = 0$ to $r = R$ was imposed radially along the base of the tank to drive horizontal convection in the z-r plane. The side wall and top surface of the tank are thermally insulated by imposing a zero normal temperature gradient on these surfaces. This is in contrast to a study done by Sheard *et al.*[8] where an aspect ratio of 0.4 was used and a free-slip condition was imposed along the top boundary.

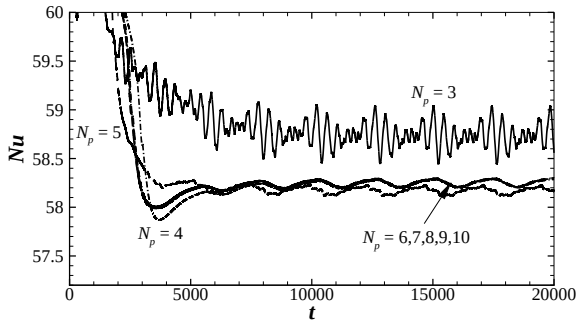

Figure 2. Time history of Nusselt number for rotating radial convection at $Ra = 10^9, Q = 20, Ro = -0.5$ with different polynomial order employed for the spectral element method. The plot has a Nusselt number range of 1 % between the lower and upper limit. It shows there is indistinguishable differences for polynomial order of 5 and above.

The incompressible Navier–Stokes equations with Boussinesq approximation are used, in which the density differences in the fluid are neglected except through the gravity term in the momentum equation. The gravity acts in the vertical z direction. The lengths are scaled by R, velocity by $R\Omega$, time by Ω^{-1}, pressure by $\rho_0 R^2\Omega^2$ (where ρ_0 is the reference density), and temperature by $\delta\theta$. With these scalings, the governing equations are written as

$$\frac{\partial \boldsymbol{u}}{\partial t} = \boldsymbol{N_u} - \boldsymbol{\nabla} p + \frac{2}{(1 - Ro\,\Lambda)\,QRa^{2/5}}\nabla^2\boldsymbol{u} + \frac{4Ra^{1/5}}{(1 - Ro\,\Lambda)\,PrQ^2}\theta\hat{\boldsymbol{e}}_z, \tag{1}$$

$$\boldsymbol{\nabla}\cdot\boldsymbol{u} = 0, \tag{2}$$

$$\frac{\partial \theta}{\partial t} = N_\theta + \frac{2}{(1 - Ro\,\Lambda)\,Pr\,QRa^{2/5}}\nabla^2\theta, \tag{3}$$

where advection and convection operators are defined as $\boldsymbol{N}_u = -(\boldsymbol{u}\cdot\nabla)\boldsymbol{u}$ and $N_\theta = -(\boldsymbol{u}\cdot\nabla)\theta$, respectively. The symbol $\hat{\boldsymbol{e}}_z$ is a unit vector in the z-direction.

A number of dimensionless parameters characterise the rotating flow, including the Rayleigh number Ra, the rotation parameter Q and the Rossby number Ro. These are defined as

$$Ra = \frac{g\alpha\delta\theta R^3}{\nu\kappa_T}, \qquad Q = \frac{2\bar{\Omega}R^2}{\nu Ra^{2/5}}, \qquad Ro = \frac{R\Omega_d}{2\bar{\Omega}H}, \tag{4}$$

where $\bar{\Omega} = \Omega + \Omega_d/2$ is the mean rotation rate, g is the gravitational acceleration, α is the volumetric expansion coefficient, ν is the kinematic viscosity and κ_T is the thermal diffusivity.

The governing equations (1)-(3) are solved with an in-house solver, which uses high order spectral element method for spatial discretisation and a third-order time integration scheme based on backward-differencing. This code had been validated in a number of studies on natural convection with Boussinesq approximation in Cartesian and cylindrical coordinate systems [7, 5].

The computational domain in the z-r plane was discretised into quadrilateral elements. A rectangular mesh comprising 2700 elements was constructed to discretise the meridional semi-plane. This is illustrated in figure 1. In order to resolve the flow accurately, the grid size was much smaller in the vicinity of the side and bottom walls, particularly the heated boundary, with coarser grid spacing in the interior. A grid resolution study was undertaken to determine a suitably accurate element polynomial

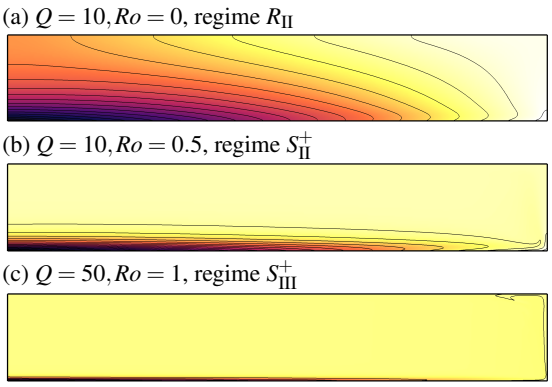

Figure 3. Contour plots of temperature at different positive Rossby number where the heated surface rotates faster than the tank rotation, for Rayleigh number $Ra = 10^9$, plotted on a meridional plane through the center of the cylindrical tank with a symmetry axis at the left of each frame. Contour level ranges from -0.5 (dark shading) to 0.5 (light shading) denote cooler and hotter fluid respectively.

degree. A test was performed at a convective range of this study, $Ra = 10^9$, $Q = 20$ and $Ro = -0.5$ as a stringent test of the mesh resolution. A linear temperature profile varying from $\theta = -0.5$ (cooling) to $\theta = 0.5$ (heating) applied radially along the base of the cylindrical tank.

Figure 2 shows time history of Nusselt number for rotating radial convection at $Ra = 10^9, Q = 20, Ro = -0.5$ with different polynomial order employed for the spectral element method. As the interior of the tank adjusted to the moving heated boundary, the Nusselt number converged to a time-periodic value for each of the polynomial order. There are differences in Nusselt number between $N_p = 3$ and the rest of the polynomial orders. However, the differences diminished rapidly for $N_p \geq 4$; for optimum accuracy and computational cost, $N_p = 6$ was chosen for the current investigation.

Result and Discussion

Flow Structure in the Steady and Unsteady Regimes

Axisymmetric solutions were obtained by solving equations (1)-(3) using an in-house spectral element solver. The solutions were simulated at $Ra = 10^9$ for rotation parameters up to $Q = 100$ and Rossby number ranges from -1 to 1. In the case of $Ro = 0$, where there is no differential rotation between the base and the tank, all flows saturated to a time-steady state. Figure 3(a) shows a temperature contour of horizontal convection flow with a moderately strong rotation of $Q = 10$, $Ro = 0$. The rotation suppresses the horizontal convective process to form a thick thermal boundary layer which can be seen along the heated base of the enclosure. Within this thermal boundary layer isotherms slants away from the axis of rotation, whereas further from the base the isotherms slant back towards the axis to occupy most of the enclosure except for a region near the colder end of the tank. In this region, a stable thermal stratification similar to those planar horizontal convection is observed. This regime is denoted as R_{II} which corresponds to regime II of a rotation-affected mixed regime in [8]. The dynamics and stability of these flows ($Ro = 0$) have been systematically studied by Sheard *et al.* [8]. The current paper will focus on non-zero Rossby number.

When the heated base rotates faster than the main tank, a layer of faster-moving fluid is created adjacent to the moving base, this gives rise to a stronger radially outward Coriolis force

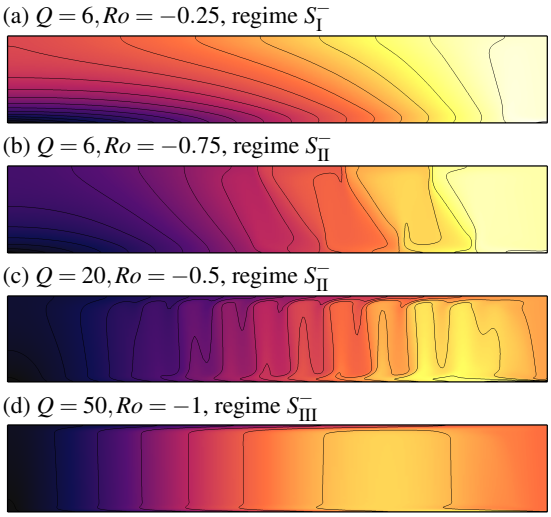

Figure 4. Contour plots of temperature at different negative Rossby number where the heated surface rotates slower than the tank rotation, for Rayleigh number $Ra = 10^9$. The same contour level is used as in figure 3.

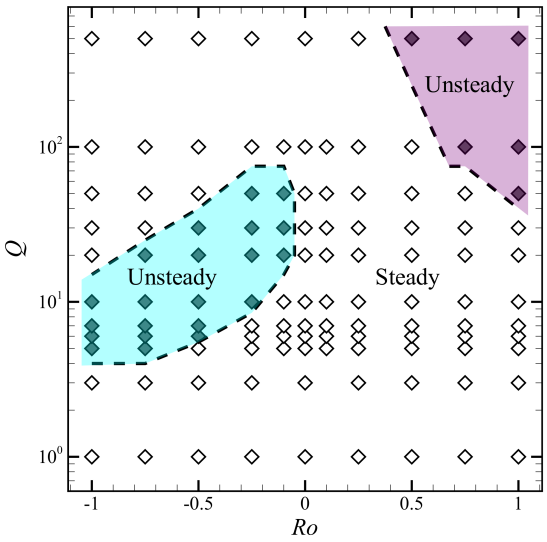

Figure 5. Flow regimes in the Rossby-Q parameter space. Two dashed curves are included for guidance to delineate the time-dependent and time-independent regimes. The unsteady counter-rotating regime is shaded with light green, whereas the unsteady co-rotating regime is shaded with light purple.

which compels the fluid to move radially toward the edge of the tank. This radially outward movement of fluid is in the same direction as the thermal gradient, it is called thermally direct mechanical forcing [4]. The effect of this is to enhance the horizontal convective process and counter the rotation effect of the main tank. This is illustrated in figure 3(b), all the slanting isotherms have been suppressed and the flow is returned to a thermally stratified planar horizontal convection state over the whole enclosure with a steady thermal plume rises along the right edge of the tank. The thermal boundary layer is noticeably thinner, this is denoted as regime S_{II}^{+}, where the $+$ superscript indicates the heated base rotates faster than the main tank. At $Q = 50$ and $Ro = 1$, a stronger thermally direct forcing produces an unsteady thermal plume, it moves along the edge and the top surface of the tank. This plume interacts with colder fluid along the top surface and entrances colder fluid into the interior of the enclosure. This circulation is confined to the hot end of the tank, within a thin thermal boundary layer along the edge and the top boundary as seen in figure 3(c). This entrancement of the colder fluids at the top is responsible for time-dependence flows in this S_{III}^{+} regime.

For negative Rossby number, the heated base rotates slower than the main tank. This creates a layer of slower moving fluids adjacent to the heated base results in a force opposing to the radial thermal gradient, this is called thermally indirect mechanical forcing. The radially inward force suppresses the formation of the thermal plume at the end-wall. When the indirect forcing overcame the thermal gradient, the flow is reversed and moving hotter fluids against the thermal gradient in a clockwise direction to form a small circulation cell near the edge of the tank as depicted in figure 4(a) for $Q = 6$, $Ro = -0.25$. This is denoted as regime S_{I}^{-}. Figure 4(b) shows three circulation cells incline at an angle of 45° as rotation rate of the heated base is reduced to $Ro = -0.75$. Erosion of stable stratification at the center of the tank is observed as isotherms are inclined at a steeper angle. Figure 4(c) present temperature contour for $Q = 20$, $Ro = -0.5$. Since the Rossby number is related to the rotation parameter, Q, in this case, the difference between the tank and the base rotation is in fact much greater than for the case of $Q = 6$, $Ro = -0.5$. This leads to the formation of multiple circulation cells with vertical isotherms within the enclosure. Furthermore, these circulation cells are time-dependence, like a travelling wave radiating outward to the edge of the tank. This is classified as unsteady regime S_{II}^{-}. When the rotation parameter is increased to $Q = 50$ with a Rossby number of $Ro = -1$, this creates a strong differential rotation rate where the tank rotation dominates over the rotating base. This can be seen in figure 4(d), the interior of the enclosure is dictated by the tank rotation where the flows are essentially two-dimensional with columnar temperature fields. The effect of the heated rotating base is to move hotter fluids to the inner part of the enclosure, depicted as lighter (hotter) contour region in figure 4(d). The flow is steady, this regime is denoted as S_{III}^{-}.

The results demonstrate two distinct unsteady regimes amongst the time-independent flows within the parameter space as depicted in figure 5. These unsteady regimes are S_{III}^{+} and S_{II}^{-}. In the case of positive Rossby number (where heated base rotates faster than the tank), the unsteady dynamics are governed by the heated rotating base. The faster-rotating base induces radially outward flow along the base to enhance horizontal convection. The resulting unsteady flow is similar in nature to planar horizontal convection at high Rayleigh number where unsteadiness is attributed to plume eruption from the thermal boundary layer. On the other hand, when the heated base rotates slower than the tank, the time-dependence behaviours are more complex. It arises from competition between the thermal gradient along the heated base and an imbalance of Coriolis forces from the differential rotation. This unsteadiness is characterised by travelling thermal waves moving radially outward toward the hot end of the enclosure.

Nusselt Number Scalings

The heat transfer through the moving base of the cylindrical tank is considered. A horizontal Nusselt number is used as a measure of heat transfer. The effect of rotation is to suppress horizontal convection in the z-r plane [8], which leads to a reduction in the Nusselt number depicted in figure 6 as a red solid line. The Nusselt number decreases to a constant value at high Q.

For positive Rossby number, horizontal convection is enhanced

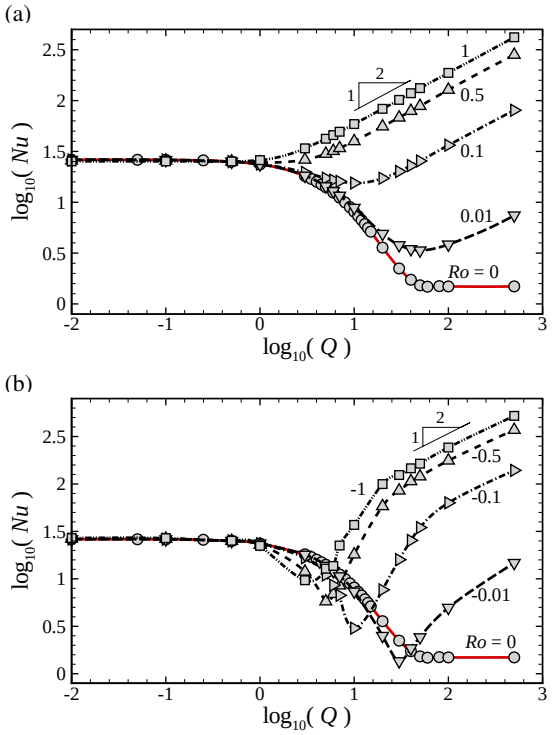

Figure 6. A plot of base-10 logarithmic of Nusselt number, Nu, against rotation parameter, Q, for different value of (a) positive and (b) negative Rossby number, Ro as indicated in the figure. A gradient of $1/2$ is included for visual guidance of the Nusselt number scaling.

due to radially outward flows created by a faster moving base. The increase of Nusselt number is shown in figure 6(a), which scales with $\sim Q^{1/2}$ at high rotation parameter and Rossby number.

On the other hand, with negative Rossby number, the heat transfer was initially suppressed due to the thermally indirect forcing, where the radially inward flows are opposing the thermal gradient. As soon as the thermal gradient had been overcome to form an internal clockwise circulation cell, the Nusselt number begins to increase as illustrated in figure 6(b). The Nusselt number eventually reaches a scaling of $\sim Q^{1/2}$ at high Rossby number. At low differential rotation rates, the Nusselt number scaling is controlled by natural convection and by Ekman pumping at high differential rotation rates.

Conclusion

The effects of a heated moving surface on rotating horizontal convection is systematically investigated using a high resolution in-house spectral element code. The flow structures, regimes map, and heat transfer scaling are presented.

In conclusion, the current study illustrates that for a positive Rossby number (where the base rotates faster than the tank), the flow exhibits characteristics of a classical planar horizontal convection flow with plumes extending upward at the side wall. On the other hand, for a negative Rossby number, the surface shear stresses carry heat toward the interior of the tank thus creating multiple circulation cells within the enclosure.

It is established that thermally direct forcing (positive Rossby number) enhance heat transfer via end-wall plume through a thermal boundary layer along the heater base. The thermally indirect forcing carries heat through multiple circulation cells which enhance the Ekman pumping in transferring heat into the interior of the tank. The results show the Nusselt number scales with $\sim Q^{1/2}$ for all Rossby numbers at high Q values.

This research highlights the pivotal role plays by the surface shear stresses in enhancing the heat transfer of rotating horizontal convection.

Acknowledgement

This research was supported by Australian Research Council through Discovery Grant DP120100153, DP150102920 and DP180102647, and was undertaken using high-performance computing resources from the National Computational Infrastructure (NCI) thanks to a grant under the National Computational Merit Allocation Scheme (NCMAS). NCI is supported by the Australian Government.

References

[1] Barkan, R., Winters, K. B. and Llewellyn Smith, S. G., Rotating horizontal convection, *Journal of Fluid Mechanics*, **723**, 2013, 556–586.

[2] Barkan, R., Winters, K. B. and Llewellyn Smith, S. G., Energy cascades and loss of balance in a reentrant channel forced by wind stress and buoyancy fluxes, *Journal of Physical Oceanography*, **45**, 2015, 272–293.

[3] Beardsley, R. C. and Festa, J. F., A numerical model of convection driven by a surface stress and non-uniform horizontal heating, *Journal of Physical Oceanography*, **2**, 1972, 444–455.

[4] Hazewinkel, J., Paparella, F. and Young, W., Stressed horizontal convection, *Journal of Fluid Mechanics*, **692**, 2012, 317–331.

[5] Hussam, W. K., Tsai, T. and Sheard, G. J., The effect of rotation on radial horizontal convection and Nusselt number scaling in a cylindrical container, *Int. J. Heat Mass Tran.*, **77**, 2014, 46–59.

[6] Ilıcak, M. and Vallis, G. K., Simulations and scaling of horizontal convection, *Tellus A: Dynamic Meteorology and Oceanography*, **64:1**, 2012, 18377.

[7] Sheard, G. and King, M., Horizontal convection: Effect of aspect ratio on rayleigh number scaling and stability, *Applied Mathematical Modelling*, **35**, 2011, 1647–1655.

[8] Sheard, G. J., Hussam, W. K. and Tsai, T., Linear stability and energetics of rotating radial horizontal convection, *Journal of Fluid Mechanics*, **795**, 2016, 1–35.

[9] Stewart, K. D., Hughes, G. O. and Griffiths, R. W., The role of turbulent mixing in an overturning circulation maintained by surface buoyancy forcing, *Journal of Physical Oceanography*, **42**, 2012, 1907–1922.

[10] Vallis, G. K., Large-scale circulation and production of stratification: Effects of wind, geometry, and diffusion, *Journal of Physical Oceanography*, **30**, 2000, 933–954.

[11] Vreugdenhil, C. A., Griffiths, R. W. and Gayen, B., Geostrophic and chimney regimes in rotating horizontal convection with imposed heat flux, *Journal of Fluid Mechanics*, **823**, 2017, 57–99.

[12] Whitehead, J. and Wang, W., A laboratory model of vertical ocean circulation driven by mixing, *Journal of Physical Oceanography*, **38**, 2008, 1091–1106.